Water Research 167 (2019) 115032

Contents lists available at ScienceDirect

Water Research

journal homepage: www.elsevier.com/locate/watres

Full-scale investigation of in-situ iron and alkalinity generation for efficient sulfide control

Ilje Pikaar [a, b, *], Markus Flugen [a], Hui-Wen Lin [c], Sirajus Salehin [a, b], Jiuling Li [b], Bogdan C. Donose [d], Paul G. Dennis [e], Lisa Bethke [b], Ian Johnson [f], Korneel Rabaey [b, g], Zhiguo Yuan [b]

[a] The University of Queensland, The School of Civil Engineering, QLD, 4072, Australia
[b] The University of Queensland, Advanced Water Management Centre (AWMC), QLD, 4072, Australia
[c] Department of Agricultural Chemistry, National Taiwan University, Taiwan" to "Department of Agricultural Chemistry, National Taiwan University, Taipei, Taiwan
[d] The University of Queensland, School of Chemical Engineering, St. Lucia, QLD, 4072, Australia
[e] The University of Queensland, School of Earth and Environmental Sciences, QLD, 4072, Australia
[f] The City of Gold Coast, 833 Southport Nerang Road, Nerang, QLD, 4211, Australia
[g] Center for Microbial Ecology and Technology (CMET), Ghent University, Coupure Links 653, 9000, Ghent, Belgium

ARTICLE INFO

Article history:
Received 12 April 2019
Received in revised form
27 August 2019
Accepted 28 August 2019
Available online 5 September 2019

Keywords:
Hydrogen sulfide abatement
Electrochemistry
Real-life application
Sewer corrosion
In-situ chemical generation

ABSTRACT

Hydrogen sulfide induced corrosion of concrete sewer pipes is a major issue for wastewater utilities globally. One of the most commonly used methods to combat hydrogen sulfide is the addition of ferric chloride. While a reliable and effective method, ferric chloride is acidic causing OH&S concerns as well as alkalinity consumption in sewage. This study investigates, under full-scale field conditions, an alternative method for sulfide control by in-situ electrochemical generation of iron ions using sacrificial iron electrodes. This method concomitantly produces alkalinity through cathodic OH^- generation, rather than consumption. The gaseous hydrogen sulfide concentrations at the discharge wet well of a real-life rising main (length: ~1 km in, diameter: 150 mm) decreased from 173 ppm to 43 ppm (90 percentile of peak values), when a current of 0.86 A/m^3 of sewage was applied. The 90 percentile peak H_2S value was further reduced to 6.6 ppm when the applied current was increased to 1.14 A/m^3 sewage. Moreover, methane generation was almost completely inhibited from 25.3 ± 1.46 mg COD/L to 0.06 ± 0.04 mg COD/L. The overall cell voltage remained constant throughout the experimental period clearly showing the stability of the process. Detailed characterization of the down-stream sewer pipe biofilm revealed the complexity of the iron chemistry as the in-situ produced iron ions undergo transformation into a variety of iron species. Overall, this study demonstrates that in-situ generation of iron and alkalinity is an effective alternative method for hydrogen sulfide control in sewers.

© 2019 Published by Elsevier Ltd.

1. Introduction

Hydrogen sulfide induced corrosion of concrete sewer pipes is a major issue for water utilities worldwide (Hvitved-Jacobsen et al., 2013; Pikaar et al., 2014). Current methods typically implemented by the water industry for sulfide control predominantly rely on the continuous addition of chemicals including oxygen, caustic soda, magnesium hydroxide, sodium nitrate, and iron salts (Ganigue et al., 2011; Jiang et al., 2015a; Zhang et al., 2008). One of the most commonly used chemicals are iron salts, either in the form of ferrous ($FeCl_2$) or ferric chloride ($FeCl_3$), to precipitate sulfide as iron sulfide (Ganigue et al., 2011; WERF, 2007). It is considered a proven and robust sulfide control method that has been implemented by the water industry for several decades (WERF, 2007). Moreover, very high removal efficiencies can be obtained with achievable dissolved sulfide concentrations of well below 1 mg/L (Firer et al., 2008; Nielsen et al., 2005). More recently, in addition to its capability to precipitate sulfide to low concentrations, some laboratory scale studies revealed that the addition of iron resulted in a substantial decrease (i.e. up to 60%) in the sulfide production

* Corresponding author. The School of Civil Engineering, The University of Queensland, St. Lucia, QLD, 4072, Australia.
E-mail address: i.pikaar@uq.edu.au (I. Pikaar).

https://doi.org/10.1016/j.watres.2019.115032
0043-1354/© 2019 Published by Elsevier Ltd.

rate (Zhang et al. 2009, 2012), thereby lowering the overall chemical requirements. In these studies, methanogenic activity was also found to be inhibited by 40–80%. It was hypothesized that sulfate reducing bacteria (SRB) and methanogens were inhibited by iron compounds, although the exact mechanisms behind these substantial reductions could not be elucidated.

Despite the above mentioned characteristics and advantages of iron salts dosing, its use also comes with several drawbacks. First, the transport, handling and storage of highly corrosive and strongly acidic iron salts (e.g. $pKa = Fe(H_2O)_6^{3+}$ is 2.20) is associated with Occupational Health and Safety (OH&S) concerns and requires special materials for the delivery and storage tanks to meet safety and regulation requirements (WERF, 2007). In fact, in some urban locations it is not even allowed for iron salts (and often chemicals in general) to be stored on-site (personal communication with water utilities). Secondly, the strong acidic nature (Brezonik and Arnold, 2011; Cornell and Schwertmann, 1996) of ferric salts and ferrous salts (after oxidation of ferrous to ferric), consumes alkalinity and results in decrease of the sewage pH. While this reduction in pH might not be that substantial in absolute terms, it has a significant impact on iron dosing requirements, especially around the circumneutral pH values often observed in sewers. For example, Firer et al. (2008) found that in order to achieve the same effluent sulfide concentration of 0.1 mg S/L, the required iron dosing increases by about 200% when the pH of sewage was decreased from 7.0 to 6.5.

To overcome the above mentioned drawbacks of conventional iron salts dosing, we recently proposed an alternative method that allows for in-situ electrochemical generation of ferrous (Fe^{2+}) ions from sewage using iron plates as sacrificial anodes (Lin et al., 2017b). During both short-term and long-term laboratory scale experiments, the feasibility was successfully demonstrated. This study showed that Fe^{2+} can be generated in-situ in sewage at very high Coulombic efficiencies (i.e. >95%), whereas long-term experiments showed that sulfide was efficiently removed at an average removal efficiency of $95.4 \pm 4.4\%$ over a period of 8 weeks.

A key advantage was found to be a slight increase in sewage pH due to concomitant alkalinity generation through cathodic OH^- formation, contrarily to the acidifying effect of conventional iron salts dosing. Moreover, it was found that the formation of solids aggregates, normally observed during conventional electrocoagulation (Mollah et al., 2001; Sahu et al., 2014; Vong and Garey, 2014), could be avoided by applying low current densities and by minimizing the mixing intensity (Lin et al., 2017b). Competing anodic reactions like oxygen evolution and direct sulfide oxidation at the electrode surface were completely avoided with the oxidation of iron to ferrous ions being the only anodic reaction taking place due to the low anode potentials (Lin et al., 2017b).

While the above studies highlighted the working principle and potential of electrochemical iron oxidation and alkalinity generation, the performance, in terms of sulfide control under real sewer conditions, was not investigated. The experiments were conducted under controlled laboratory conditions using a small-size (600–750 mL) continuously stirred tank reactors (CSTR). The conditions in sewers are fundamentally different as a sewer pipe is more like a plug-flow reactor than a CSTR. Secondly, the flow is often characterized by large variations in sewage flow rate following a diurnal pattern. The latter has enormous impact on the sulfide production rates resulting in highly dynamic hydrogen sulfide profiles (Sharma et al. 2008, 2013). Finally, several engineering challenges when scaling-up the technologies from laboratory scale to full-scale implementation can be expected. For example, our previous study highlighted the importance of minimizing the applied current density and inter-electrode gap in order to minimize the voltage losses caused by the ohmic drop. However, in real-life application in sewers, the use of a small inter-electrode gap may cause blockages.

In this study, we aim to investigate the feasibility and long-term performance of electrochemical oxidation of iron and alkalinity generation for efficient sulfide control in sewers through real-life application. To assess the performance in terms of sulfide control efficiency and electrochemical stability of the process, the cell voltage of the electrochemical cell as well as the gaseous hydrogen sulfide concentration in the receiving wet well at the end of the sewer were continuously monitored, enhanced by manual sampling and off-line analysis of liquid period parameters in order to investigate the potential impact on SRB and methanogenic activity. Moreover, the fate and chemical transformations of the produced iron ions was also investigated by detailed characterization of the down-stream sewer biofilm.

2. Material and methods

2.1. The full-scale sewer site

The electrochemical system, described in the next sub-section, was placed at the pumping station of the UC09 rising main sewer (Blueash Crescent, Oxenford QLD 4210O, Queensland, Australia). The sewer pipe has a length of 1080 m with an inner diameter of 150 mm (see Fig. 1 and Fig. S1) and receives sewage from a residential area. The submerged pumps inside the pumping station wet well, operated by Gold Coast City Council, were operated in intermittent mode. Once the water level in the wet well reached 19.5% (high level) of the total height of the wet well, a pump is turned on until the water level drops to 3.5% (low level). The sewage pumped in each pump run is estimated to be 3.9 m^3. Under normal dry weather conditions, there are on average 43 pumping events per day equalling to an average dry weather daily flow of ~140 m^3/day. The flow in dry weather follows a typical diurnal pattern resulting in a HRT ranging between 3 and 7 h, depending on the time of the day, as previously reported (Jiang et al., 2013). During wet weather, the sewage flow increases substantially (see Figs. S3A–F), resulting in much shorter HRTs with the lowest close to <1 h.

2.2. The electrochemical cell and operation

The electrochemical cell (and other peripherals) was placed within a 20 ft container (Fig. 1, Fig. S2) (Nijhuis Water Technologies, Doetinchem, The Netherlands). Sewage was continuously pumped from the wet well (6 m deep) into the electrochemical cell at a flow rate of 12.5–16.5 m^3/hour using a grinder pump (ABS Piranha grinder pump, Sulzer, Switzerland). The flow fluctuated depending on the water level in the wet well, as well as the level of solids and debris in the wastewater. The effluent of the electrochemical cell was subsequently fed back into the wet well by means of gravity.

The electrochemical cell consisted of two rows of 50 carbon steel plates each with a weight of ~19 kg and a dimension of 1 cm × 60 cm × 40 cm. The carbon steel plates were placed within the cell with an inter-electrode gap of 3 cm. The latter distance was chosen in order to prevent potential blockages as the grinder pump 'cuts' solids into pieces smaller than 3 cm as well as to minimize formation of ragging over time (personal communication Nijhuis Water Technology). Each row, which comprised 50 carbon plates, was galvanostatically controlled using separate power sources (E Amstel 3, Amstel rectifiers, The Netherlands). Depending on the experimental period, the current supplied to each row was 0, 40, 80 or 100 A, respectively equalling to a total applied current of 80, 120 and 160A in the three experimental periods (P1–P3), respectively (see section 2.3). Considering a total anode surface of ~12 m^2 for each row, the applied current density equalled to 3.3–8.3 A m^{-2}. To allow for equal dissolution of the sacrificial electrodes, polarity

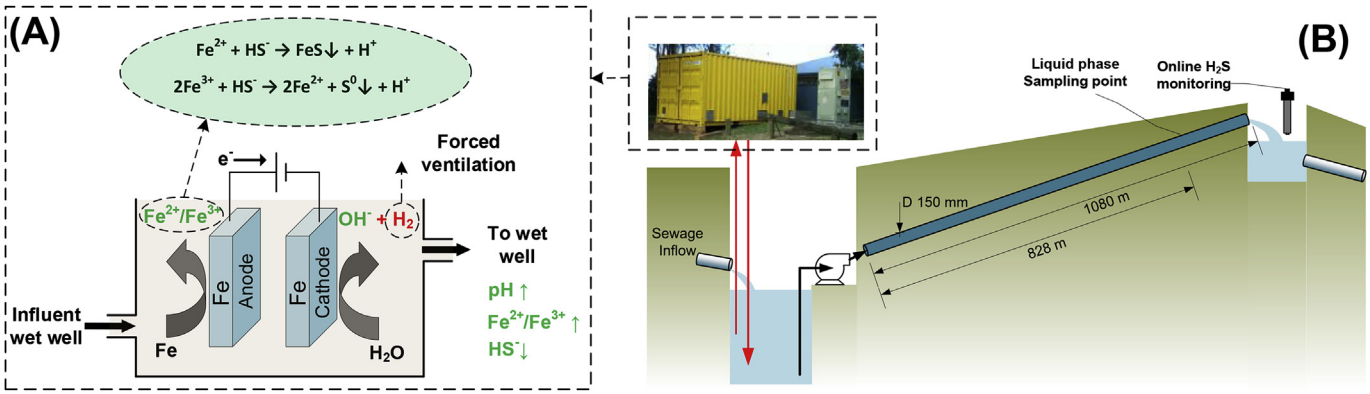

Fig. 1. (A) Conceptual reactions within the electrochemical cell and (B) Schematic of the UC09 rising main and the electrochemical installation at its pumping station.

switching (i.e. the anode becomes cathode and vice versa) was automatically applied every 2 h). The electrochemical cell was covered with a Polyvinylchloride (PVC) lid with two transparent acrylic observation windows (see Fig. S2). Forced ventilation was continuously applied to the headspace of the reactor using air blowers to ensure that the produced hydrogen gas concentration was well below the lower explosive level (i.e. 4%). Once per week, the electrochemical cell was drained and flushed for 30 min to minimize build-up of larger size particles and rags on the bottom of the cell.

2.3. Experimental protocol

The experiments were divided into three periods, namely (i) the baseline period, (ii) the experimental period and (iii) the post-experimental period (see Table 1).

(i) The baseline period lasted for 7 weeks. This period was included to determine the hydrogen sulfide concentrations in the gas phase in the discharge wet well as well as the liquid period sulfide and methane concentrations, in the absence of electrochemical iron dosing.

(ii) The experimental period lasted for 14 weeks (99 days), during which the cell was operational. This period was further divided into three periods in which different total currents were supplied: (P1) 80 A (~6.5 weeks; 46 days), (P2) 120 A (~3 weeks; 21 days) and (P3) 160 A (~4 weeks; 28 days). These currents corresponded to an iron dosing rate of 14, 21 and 28 mg Fe per liter of sewage, assuming a coulombic efficiency of 100% for the oxidation of Fe to Fe^{2+} (see supplementary information for more details on the calculations used) and an average dry weather flow of 140 m^3/day.

(iii) The post-experimental period lasted for 6 weeks. It was conducted in order to assess how quickly the gaseous hydrogen sulfide concentration would return to the baseline levels. In addition, the fate and transformations of the *in-situ* produced iron ions as well as the microbial community were investigated by analyzing the chemical and microbial composition of the sewer biofilm (see Supplementary Information).

2.4. Monitoring and sampling

A hydrogen sulfide sensor was placed 50 cm above the water level in the discharging wet well (Fig. 1), which enabled continuous (logged every 60 s) monitoring of the gaseous hydrogen sulfide concentration in the headspace of the wet well. The sensor was calibrated every 4 weeks with a 50 ppm hydrogen sulfide calibration gas (Calgaz Standard 50PPM H2S, Balance AIR), which confirmed that sensor drift did not occur.

The overall cell voltage of each of the power sources were monitored online every 5 min using a National Instruments Compact RIO Controller-9066 with NI 92018 AI, ±10 V, 12 Bit, 500 kS/s Aggregate input module. The diurnal variation in sewage flow and consequently fluctuations in the hydraulic retention time, as well as the impact of rain events were assessed based upon

Table 1
Experimental periods, monitoring and sampling points.

Experimental periods	Current applied (Ampere)	Liquid analysis (grab samples and 24 h composite sampling)		Online monitoring	Analysis sewer biofilm
		Inlet of rising main	828 m downstream of rising main inlet	Discharging wet well outlet rising main	828 m downstream of rising main inlet
Baseline (week 0–7)	0 A	Dissolved sulfur species (i.e. sulfide, sulfite, thiosulfate and sulfate), volatile fatty acids, iron (total and dissolved), dissolved methane, pH and temperature.		Hydrogen sulfide sensor, measuring every 60 s.	N/A
Experimental (week 8–22)	80 A (week 8–15) 120 A (week 16–19) 160 A (week 20–24)				
Post-experimental (week 23–28)	0 A				X-ray Powder Diffraction (XRD), Scanning Electron Microscopy/Energy Dispersive X-ray Spectroscopy (SEM/EDS), Microbial analyses.

SCADA data, which recorded the pump on/off time. The method reported in (Chen et al., 2014) was used to calculate the sewage flow using the SCADA data.

A sampling point was placed at the pumping station as well as 828 m downstream of the inlet of the rising main (Fig. 1). These sampling points were used to take grab samples for analysis of the dissolved sulfur species (i.e. sulfide, sulfite, thiosulfate and sulfate), volatile fatty acids, iron (total and dissolved), dissolved methane, pH and temperature. 24 h composite sampling (ISCO 3710 portable composite sampler) was also conducted at the downstream sampling point to determine the fluctuations and actual iron concentration in the sewage caused by daily variation in sewage flow.

On the first day of the post-treatment period, a section of the sewer pipe with a length of 600 mm, located at the sampling point 828 m downstream of the pumping station, was removed from the rising main and replaced with a new pipe section. The section was immediately filled with fresh sewage to maintain real sewer conditions thereby maintaining the integrity of the biofilm. The pipe section was subsequently transported to the laboratory where biofilm samples were immediately frozen and stored at −80 °C. Prior to X-ray Powder Diffraction (XRD) and Scanning Electron Microscopy/Energy Dispersive X-ray Spectroscopy (SEM/EDS) analyses, samples were freeze-dried overnight and the resulting powder was immediately analyzed. DNA was extracted from 250 mg of thawed sewer biofilm using the Power Soil DNA Isolation kit (MO BIO Laboratories, Carlsbad, CA) according to the manufacturer's recommendations (see Supplementary Information for more information).

2.5. Analytical methods

Dissolved sulfur species (i.e. sulfide, sulphite, thiosulfate and sulfate) were measured using Ion Chromatography equipped with a Dionex 2010i system (Keller-Lehmann et al., 2006). The pH and temperature of the sewage was measured using a hand-held pH meter (Hanna Instrument, USA). Total and dissolved iron concentrations (i.e. Fe^{2+} and Fe^{3+}) as well as other cations and anions such as Na^{+}, Mg^{+}, Ca^{2+}, PO_4^{3-}, and SO_4^{2-} were measured using inductively coupled plasma optical emission spectrometry (ICP-OES, 7300DV, PerkinElmer, USA). To measure the dissolved iron concentrations, samples were pre-filtered with a 0.22 μm membrane filters prior to analysis. The protocol used to determine the dissolved methane concentrations is described in detail elsewhere (Alberto et al., 2000; Guisasola et al., 2008). In summary, 5 mL of sewage was immediately filtered using a 0.22 μm membrane filters and injected into an evacuated into an Exetainer® tube (Labco, UK) with a volume of 12 mL. The sample was subsequently kept for 24 h in order for the gas and liquid period methane concentrations to reach equilibrium. The gas period methane concentration was subsequently measured using a gas chromatography (GC) equipped with a flame ionization detector, thereby allowing to calculate the liquid period methane concentration in the sewage using Henry's law. The volatile solids to total solids ration (i.e. the VS/TS ratio) of the sewer biofilm was analyzed using Standard Methods 2540D and 2540E, respectively (APHA, 1995). Volatile fatty acids (VFAs) were analyzed using a gas chromatograph equipped with a flame ionization detector and a capillary column (Agilent 7890A, DB-FFAP 125−3212).

XRD and SEM/EDS analyses were carried out to investigate the fate and potential transformation of the in-situ produced iron ions in the sewage by analysing the sewer pipe biofilm at the downstream sampling point. X-ray diffractograms were recorded with a D8 Bruker diffractometer using a Cu $K_{\alpha 1}$ radiation at $\lambda = 1.55$ Å. SEM/EDS measurements were done using a Hitachi SU3500 Scanning Electron Microscope equipped with Oxford Instruments X-Max SDD x-ray detector enabling simultaneous imaging and elemental analysis at high count rates with 125eV energy resolution.

3. Results and discussion

3.1. Hydrogen sulfide control performance

Fig. S4 shows a 24h gaseous H_2S profile measured on a typical dry weather day in the baseline period, along with pumping events on the day. The wastewater discharge to the wet well, induced a pumping event, caused an immediate rise of the gaseous H_2S concentration. The H_2S concentration then dropped gradually, likely due to the draining of the wastewater from the wet well to the downstream gravity pipe, until the next pumping event. The magnitudes of the peaks are directly associated with the dissolved sulfide concentration in wastewater, while the receding parts of the H_2S profiles are more related to the hydraulics. Therefore, an important indicator of the effectiveness of any sulfide strategies is the reduction of peak H_2S levels.

With the above described method, H_2S peak values were identified from the H_2S raw data measured during the entire experimental data (see Fig. 2A−E). It can be seen that during the baseline as well as the post-treatment period hydrogen sulfide concentrations followed a similar pattern with the highest hydrogen sulfide concentrations observed in the morning (6−8 am), consistent with previous reports (Jiang et al., 2013). This is because that wastewater flow is lower at night time, resulting in longest retention time of slugs discharged to the wet well in the early morning. For a similar reason, relatively higher H_2S values were also observed in late afternoon and evening.

Fig. 2A−E clearly shows that the H_2S concentrations were substantially reduced with the commissioning of the electrochemical cell. When a current of 80 A was applied in P1, the H_2S concentrations were reduced to levels lower than 10 ppm for most of the time in a day. However, the morning peaks reached 150 ppm, in comparison to 250 ppm measured in the baseline period. With the increase in the current to 120 A and 160 A in P2 and P3, respectively, the H_2S peak values were further reduced to 80 and < 20 ppm, respectively.

Fig. 3 shows the 90 percentiles of the peak hydrogen sulfide concentrations measured during the baseline, experimental (P1−P3) and post-treatment periods. The 90%ile peak hydrogen sulfide concentrations during the baseline and post-treatment periods were similar with peak values of 173 and 197 ppm, respectively. Such high hydrogen sulfide levels are known to cause severe concrete corrosion (Jiang et al., 2015b; WERF, 2007). When a current of 0.57 A/m^3 (P1) of sewage was applied, the 90%ile peak hydrogen sulfide concentrations decreased to 92 ppm (i.e. a reduction of 54%). Increasing the current to 0.86 A/m^3 (P2) and 1.14 A/m^3 (P3) of sewage resulted in 90%ile peak hydrogen sulfide levels of 43 ppm and 6.6 ppm, respectively. The latter corresponds to a reduction in hydrogen sulfide concentrations of 75% and 96%.

The reduction in gaseous H_2S concentrations was supported by the liquid period measurement (Fig. S6). The dissolved sulfide concentrations were clearly lower ($p < 0.05$) in the experimental period (P1) than in the baseline period (Figure S6, 7.4 ± 2.3 versus 1.5 ± 1.4 mg S/L). Also, the wastewater pH was higher ($p < 0.05$) in the experimental period (P1) than in the baseline period (i.e. 8.5 ± 0.5 versus 8.0 ± 0.5). Both lowered dissolved sulfide concentrations and elevated pH would have contributed to the reduced gaseous H_2S concentrations. However, the dissolved sulfide concentrations was 4.3 mg S/L at 7am on the day of the measurement (in P1), which explains the relatively high gaseous H_2S values in the morning in P1 (Fig. 2B). The dissolved sulfide concentrations then dropped to values below 1 mg S/L, which in conjunction with

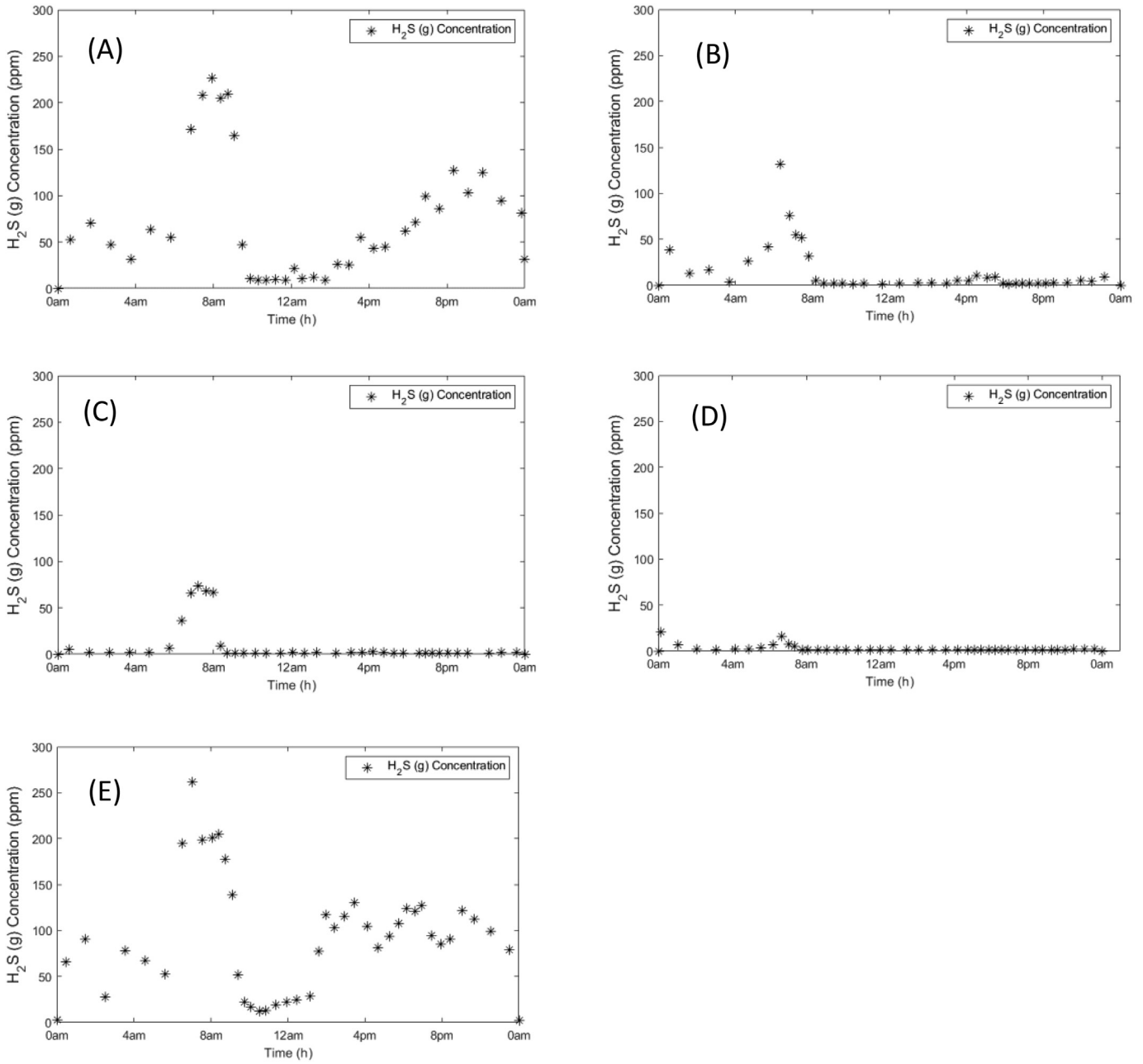

Fig. 2. Typical 24 h profile of the peak hydrogen sulfide concentration in the headspace of the receiving discharge wet well 1080 m downstream during (A) the baseline period (no current applied), (B–D) experimental period at applied currents of 80, 120 and 160 Ampère and (E) post-treatment period (no current applied). The peak hydrogen sulfide (g) profiles shown were taken from representative days during dry weather flow conditions on a week day.

elevated pH (almost 8.5), resulted in much lowered gaseous H_2S concentration for the rest of the day.

3.2. Electrochemical cell performance

Fig. 4A shows that during the course of the different experimental periods, stable cell voltages were obtained ranging between 1.86 ± 0.19 to 3.92 ± 0.4 V, depending on the current density applied. These values correspond to a power input of 0.040, 0.062, 0.082 kWh/m^3 treated at a total current input of 80, 120 and 160A, respectively. The slight fluctuations in the cell voltages that were repeatedly obtained within a 24 h cycle (see Fig. S5) can be attributed to slight fluctuations in sewage composition (e.g. pH and conductivity) due to diurnal consumption patterns. Importantly, throughout the course of the field trials, there were no signs of electrode passivation or scaling indicating that a constant electrochemical performance in terms of power requirements can be achieved and can be maintained over a long period of time without the need for electrode maintenance and replacement. While the electrochemical performance in terms of power requirements to dissolve iron ions (expressed in kg Fe) was stable, as a consequence of the constant applied current and a highly dynamic diurnal pattern in hydraulic flow under dry weather conditions, the measured total iron concentration fluctuated over time ranging between 7 and 42 mg Fe/L, depending on the time of the day (see Fig. 4B). These values are comparable with conventional iron dosing

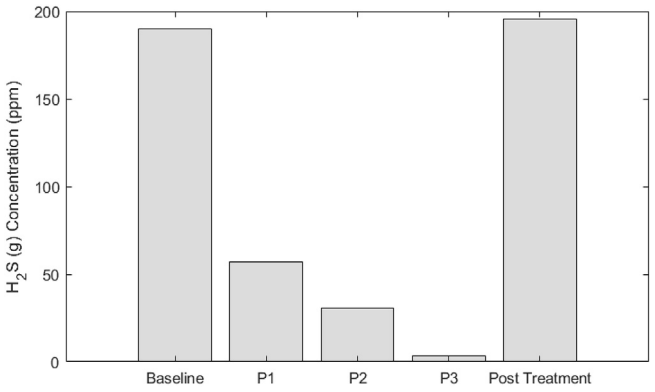

Fig. 3. 90 percentiles of the peak hydrogen sulfide levels obtained after each pumping event at the discharge well of the rising main.

as dosing iron salts at a constant rate is a commonly used chemical dosing strategy (Ganigue et al., 2011). Consequently, the process performance in terms of required current applied to the electrochemical cell in order to dissolve sufficient iron (expressed in mg Fe/L sewage) was not constant throughout a diurnal cycle.

Due to the use of a grinder pump, blockages within the electrochemical did not occur throughout the trials. However, due to the almost universal presence of solids (e.g. hair, plastics, toilet paper, cleaning tissues and other non-degradable coarse material) in sewage, ragging and build-up of solids in the bottom of the reactor could not be completely avoided. Therefore, the electrochemical cell was manually drained and flushed for 30 min once per week. The latter frequency and duration was found to be sufficient in order avoiding build-up of solids on the bottom of the reactor.

3.3. The complexity of iron chemistry in the downstream sewer biofilm

Part of the produced iron is expected to be integrated in the biofilm matrix, thereby reducing the volatile solids-to-total solids fraction of the biofilm (Zhang et al., 2012). Indeed, after three months operation, the VS/TS ratio of the sewer biofilm was found to be 0.11. The latter is substantially higher than VS/TS ratios normally observed in sewer biofilms not subjected to chemical dosing (Zhang et al., 2012), indicating that part of the produced iron oxides attached to the sewer biofilm. To characterise the iron speciation and morphology in the downstream biofilm XRD and SEM/EDS analyses were conducted. The X-ray diffractograms indicate that amorphous material was dominant in the sewer biofilm (see Fig. S7). Amongst the iron oxide species, several polymorphs of FeOOH were identified such as goethite (α-FeOOH), akaganeite (β-FeOOH), and feroxyhyte (δ-FeOOH). Others were bernalite [$Fe(OH)_3$], hematite (ε-Fe_2O_3), magnetite (Fe_3O_4), and wustite (FeO). Several studies reported on the iron speciation during electrocoagulation (Dubrawski and Mohseni, 2013; Dubrawski et al., 2015; Tsouris et al., 2001; Van Genuchten et al., 2012). These studies revealed that electrochemical iron oxidation is a very complex process in which a variety of amorphous and crystalline iron oxide species found in the biofilm can be produced electrochemically such as magnetite, hematite, akaganeite and feroxyhyte. It was however not possible to elucidate whether these were indeed in-situ generated or formed as result of chemical transformation over time (Poulton et al., 2004) once embedded within the biofilm matrix. In addition to the amorphous iron oxide species, several crystalline Fe—S and Fe—P species were also found, as indicated by their weak diffraction signals. Iron sulfide species were identified as marcasite and/or pyrite (FeS_2), mackinawite (FeS), greigite (Fe_3S_4), pyrrhotite ($Fe_{(1-x)}S_{(x=0-0.2)}$) and/or troilite (FeS). The latter is a nonstoichiometric variant of FeS, which is also called magnetic pyrite due to resemblance in color of pyrite with weak magnetic properties. In addition, traces of iron phosphate minerals were also found such as graftonite [$Fe_3(PO_4)_2$], and iron phosphide (FeP_4). SEM/EDS of multiple samples mapped at different magnifications revealed consistently similar elemental composition matrices comprised by C, O, N, Fe, S and Ca. Elements under 1%wt were found as follows: Si (0.9%), Al (0.5%), P (0.7%) Na (0.4%) Cl (0.4) and Mg (0.3%). It is worth noting that Fe and S exhibit similar atomic percentages (>3%) and that they correlate across maps. InFigure S6 (B), brighter domains of the micrograph represent areas rich in both Fe and S.

3.4. The impact on methane emissions

In addition to hydrogen sulfide control, the iron dosing also had a clear inhibitory effect on the methanogenic activity of the sewer biofilm. In fact, methane generation was almost completely inhibited with reductions in the downstream methane concentrations from 25.3 ± 1.46 mg COD/L to 0.06 ± 0.04 mg COD/L during the baseline period and the experimental period (P1), respectively

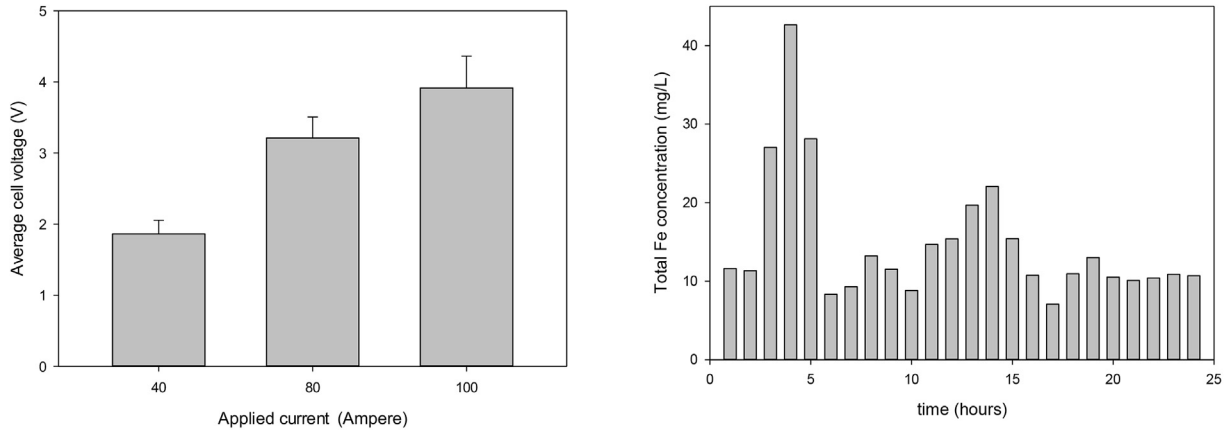

Fig. 4. (left) Average cell voltage as a function of the different applied currents during the experimental phase. Applied currents of 40, 80 and 100 Ampère correspond to current densities of 3.3, 6.7 and 8.3 A/m^2. **(right) Typical 24 h profile (from 5am to 4am) of the total iron concentration measured at the sampling point 828 m downstream of the inlet of the rising main.** The 24 h sampling was conducted on a week day under dry weather flow conditions at an applied current of 120 Ampère (P2).

(i.e. >99% reduction) (Fig. S6). This extent of inhibitions is substantially higher than that obtained during previous laboratory scale studies using ferric chloride dosing with inhibition of methanogenic activity of about 40–80% (Zhang et al. 2009, 2012). These findings are highly relevant from a practical point of view as methane (a potent greenhouse gas) emissions from sewers are considered problematic for wastewater utilities as these emission often comprise a substantial fraction of the overall carbon footprint of these utilities (Guisasola et al. 2008, 2009). Despite reduced methane emissions, a methanogenic archaeal population (genus – *Methanosaeta*) represented one of the dominant members of the biofilm communities in three of four pipe sections characterised (Fig. S8). Further research is needed to characterise the activity of this population and explain this finding.

Microbial communities also harboured sulfate reducing bacteria such as a Desulfobulbus population (Fig. S8). Contrarily to the clear impact on methane inhibition, there was no clear long-term inhibitory impact on SRB activity. In fact, peak hydrogen sulfide concentrations even slightly exceeded the levels prior to iron dosing (Fig. 3). However, it is not possible to elucidate whether iron had an inhibitory effect on the SRB activity with the available data. The HRT in the UC09 rising main ranges between 3 and 7 h. Considering these HRT values, even in the case SRB activity would be reduced, the sulfate reduction rates under these long HRTs would still result in elevated hydrogen sulfide levels at the end of the rising main.

3.5. Implications for practice

Through long-term full-scale testing this study demonstrated that electrochemical oxidation of iron and alkalinity generation through cathodic OH^- formation is a highly efficient method and represents a first step for water utilities towards electrochemical sulfide control in sewers. The 90 percentile peak hydrogen sulfide concentrations were reduced from 173 ppm (baseline) to 6.6 ppm (experimental period P3) at a current input of 1.14 A/m^3 sewage. Equally important, throughout the course of the trials, the electrochemical performance was very stable with very constant cell voltage indicating that electrode passivation caused by inorganic scaling did not take place. The process can be further optimized by applying more advanced electrical control systems. In this study, the electrochemical cell was galvanostatically controlled at fixed current inputs. As explained in section 3.2, the combination of constant current applied with a diurnal pattern in hydraulic flow under dry weather conditions, the iron concentration in the sewage was not constant (see Fig. 4B). Consequently, the required current applied to the electrochemical cell in order to dissolve sufficient iron to completely control sulfide throughout a diurnal cycle was not optimized. In a recent study, Ganigué et al. (2018) developed an on-line control algorithm for the dosing of $FeCl_3$ for sulfide control in sewers (Ganigué et al., 2018). The method involved predicting, using flow data measured on-line, sulfide formation in a sewer pipe, and determining the dosing rate based on the predicted need. The proposed method can be easily applied to the control of current in our electrochemical cell.

Based on the results obtained during this full-scale investigation, our cost calculation showed that the operational costs for electrochemical iron oxidation and alkalinity were estimated to be about 25–49.3 $/ML sewage treated (see supplementary information, Table S1). The latter clearly shows the economic competitiveness of this method as a recent industry survey revealed that chemical costs for commonly used chemicals for sulfide control implemented by the water industry range between 10.9 and 484 $/ML treated (Ganigue et al., 2011). The technology is especially interesting in situations where on-site storage of chemicals is not allowed.

To become a mature technology ready for market uptake by the water industry, the hydraulic design of the electrochemical cell needs to be further optimized. First, the electrochemical cell should either be operated continuously with automatic draining cycles. Second, the cell will need to be designed hydraulically as such that there are no 'dead' zones inside the reactor (i.e. a too low up flow velocities facilitates settling and build-up of solids). The use of Computational Fluid Dynamics (CFD) modelling will play a crucial role in achieving optimal system designs that are not prone to solid settling and build up (Rehman et al., 2017; Samstag et al., 2016).

In order to become a viable approach for larger scale sewer pipes with higher flows, it is essential to reduce the hydraulic load to the reactor. To do so, one could operate the electrochemical in semi-batch mode where only a fraction of the sewage is fed to the reactor. An alternative approach, in which the use of sewage is completely avoided, is to operate the system in batch mode using tap water. Recently, the feasibility of such an approach was demonstrated at laboratory scale by showing its working principle (Lin et al., 2017a). This study revealed that when operating in batch-mode using tap water with the addition of low levels salts it was feasible to generate a moderate strengths (i.e. ~10 g/L Fe_3O_4–Fe) solution containing magnetite nanoparticles (MNPs). Subsequent precipitation experiments showed that liquid period hydrogen sulfide concentrations can reduced to levels well below 1 mg sulfide-S/L using these MNPs. Research is currently underway investigating whether such an alternative approach could be an interesting alternative, especially for larger scale sewer pipes.

4. Conclusions

In this study, we investigated the feasibility and long-term performance of electrochemical iron oxidation with concomitant alkalinity generation for efficient hydrogen sulfide control in sewers at full-scale. The key findings of this work are:

- Electrochemical oxidation of iron and alkalinity generation can effectively control sulfide in sewers.
- A stable system performance in terms of power consumption was achieved with stable cell voltages throughout the testing period of 3 months.
- In addition to its effectiveness in controlling hydrogen sulfide, near complete inhibition of methane emissions was achieved.
- The chemistry of electrochemical oxidation and fate of iron is very complex as the in-situ produced iron ions undergo transformation into a variety of iron species found to accumulate in the sewer biofilm.

Declaration of competing interest

The authors declare that they have no known competing financial interests or personal relationships that could have appeared to influence the work reported in this paper.

Acknowledgements

This work was funded by the Australian Research Council, District of Columbia Water and Sewer Authority, ACTEW Corporation Limited, The City of Gold Coast, Queensland Urban Utilities and Yarra Valley Water through ARC Linkage project LP120200238: "In-situ electrochemical generation of caustic and oxygen from sewage for emission control in sewers". The authors acknowledge Dr. Beatrice Keller-Lehmann and Mr. Nathan Clayton for their helpful assistance with the chemical analyses. The authors acknowledge the facilities, and the scientific and technical assistance, of the Australian Microscopy & Microanalysis Research Facility at the

Centre for Microscopy and Microanalysis, The University of Queensland.

Appendix A. Supplementary data

Supplementary data to this article can be found online at https://doi.org/10.1016/j.watres.2019.115032.

References

Alberto, M.C.R., Arah, J.R.M., Neue, H.U., Wassmann, R., Lantin, R.S., Aduna, J.B., Bronson, K.F., 2000. A sampling technique for the determination of dissolved methane in soil solution. Chemosphere Global Change Sci. 2 (1), 57–63.

APHA, 1995. Standard Methods for the Examination of Water and Wastewater.

Brezonik, P.L., Arnold, W.A., 2011. Water Chemistry: an Introduction to the Chemistry of Natural and Engineered Aquatic Systems. Oxford University Press, Oxford;New York.

Chen, J., Ganigué, R., Liu, Y., Yuan, Z., 2014. Real-time multistep prediction of sewer flow for online chemical dosing control. J. Environ. Eng. 140 (11).

Cornell, R.M., Schwertmann, U., 1996. The Iron Oxides: Structure, Properties, Reactions, Occurrence and Uses. VCH, Weinheim;New York.

Dubrawski, K.L., Mohseni, M., 2013. In-situ identification of iron electrocoagulation speciation and application for natural organic matter (NOM) removal. Water Res. 47 (14), 5371–5380.

Dubrawski, K.L., Van Genuchten, C.M., Delaire, C., Amrose, S.E., Gadgil, A.J., Mohseni, M., 2015. Production and transformation of mixed-valent nanoparticles generated by Fe(0) electrocoagulation. Environ. Sci. Technol. 49 (4), 2171–2179.

Firer, D., Friedler, E., Lahav, O., 2008. Control of sulfide in sewer systems by dosage of iron salts: comparison between theoretical and experimental results, and practical implications. Sci. Total Environ. 392 (1), 145–156.

Ganigue, R., Gutierrez, O., Rootsey, R., Yuan, Z., 2011. Chemical dosing for sulfide control in Australia: an industry survey. Water Res. 45 (19), 6564–6574.

Ganigué, R., Jiang, G., Liu, Y., Sharma, K., Wang, Y.-C., Gonzalez, J., Nguyen, T., Yuan, Z., 2018. Improved sulfide mitigation in sewers through on-line control of ferrous salt dosing. Water Res. 135.

Guisasola, A., de Haas, D., Keller, J., Yuan, Z., 2008. Methane formation in sewer systems. Water Res. 42 (6), 1421–1430.

Guisasola, A., Sharma, K.R., Keller, J., Yuan, Z., 2009. Development of a model for assessing methane formation in rising main sewers. Water Res. 43 (11), 2874–2884.

Hvitved-Jacobsen, T., Vollertsen, J., Nielsen, A.H., 2013. Sewer Processes: Microbial and Chemical Process Engineering of Sewer Networks. CRC press.

Jiang, G., Keating, A., Corrie, S., O'Halloran, K., Nguyen, L., Yuan, Z., 2013. Dosing free nitrous acid for sulfide control in sewers: results of field trials in Australia. Water Res. 47 (13), 4331–4339.

Jiang, G., Sun, J., Sharma, K.R., Yuan, Z., 2015a. Corrosion and odor management in sewer systems. Curr. Opin. Biotechnol. 33, 192–197.

Jiang, G., Sun, X., Keller, J., Bond, P.L., 2015b. Identification of controlling factors for the initiation of corrosion of fresh concrete sewers. Water Res. 80, 30–40.

Keller-Lehmann, B., Corrie, S., Ravn, R., Yuan, Z., Keller, J., 2006. Preservation and Simultaneous Analysis of Relevant Soluble Sulfur Species in Sewage Samples, p. 28 (Vienna, Austria).

Lin, H.-W., Couvreur, K., Donose, B.C., Rabaey, K., Yuan, Z., Pikaar, I., 2017a. Electrochemical production of magnetite nanoparticles for sulfide control in sewers. Environ. Sci. Technol. 51 (21), 12229–12234.

Lin, H.W., Kustermans, C., Vaiopoulou, E., Prévoteau, A., Rabaey, K., Yuan, Z., Pikaar, I., 2017b. Electrochemical oxidation of iron and alkalinity generation for efficient sulfide control in sewers. Water Res. 118, 114–120.

Mollah, M.Y.A., Schennach, R., Parga, J.R., Cocke, D.L., 2001. Electrocoagulation (EC)—science and applications. J. Hazard Mater. 84 (1), 29–41.

Nielsen, A.H., Lens, P., Vollertsen, J., Hvitved-Jacobsen, T., 2005. Sulfide–iron interactions in domestic wastewater from a gravity sewer. Water Res. 39 (12), 2747–2755.

Pikaar, I., Sharma, K.R., Hu, S., Gernjak, W., Keller, J., Yuan, Z., 2014. Reducing sewer corrosion through intergrated urban water management. Science 345 (6198), 812–814.

Poulton, S.W., Krom, M.D., Raiswell, R., 2004. A revised scheme for the reactivity of iron (oxyhydr)oxide minerals towards dissolved sulfide. Geochem. Cosmochim. Acta 68 (18), 3703–3715.

Rehman, U., Audenaert, W., Amerlinck, Y., Maere, T., Arnaldos, M., Nopens, I., 2017. How well-mixed is well mixed? Hydrodynamic-biokinetic model integration in an aerated tank of a full-scale water resource recovery facility. Water Sci. Technol. 76 (8), 1950–1965.

Sahu, O., Mazumdar, B., Chaudhari, P.K., 2014. Treatment of wastewater by electrocoagulation: a review. Environ. Sci. Pollut. Control Ser. 21 (4), 2397–2413.

Samstag, R.W., Ducoste, J.J., Griborio, A., Nopens, I., Batstone, D.J., Wicks, J.D., Saunders, S., Wicklein, E.A., Kenny, G., Laurent, J., 2016. CFD for wastewater treatment: an overview. Water Sci. Technol. 74 (3), 549–563.

Sharma, K., Ganigue, R., Yuan, Z., 2013. pH dynamics in sewers and its modeling. Water Res. 47 (16), 6086–6096.

Sharma, K.R., Yuan, Z., de Haas, D., Hamilton, G., Corrie, S., Keller, J., 2008. Dynamics and dynamic modelling of H2S production in sewer systems. Water Res. 42 (10), 2527–2538.

Tsouris, C., DePaoli, D.W., Shor, J.T., Hu, M.C.Z., Ying, T.Y., 2001. Electrocoagulation for magnetic seeding of colloidal particles. Colloid. Surf. Physicochem. Eng. Asp. 177 (2–3), 223–233.

Van Genuchten, C.M., Addy, S.E.A., Peña, J., Gadgil, A.J., 2012. Removing arsenic from synthetic groundwater with iron electrocoagulation: an Fe and as K-edge EXAFS study. Environ. Sci. Technol. 46 (2), 986–994.

Vong, Y.M., Garey, D.G., 2014. Encyclopedia of Applied Electrochemistry. Springer, pp. 2117–2122.

WERF, 2007. Minimization of Odors and Corrosion in Collection Systems Phase 1. Water Environment Research Fundation, London, UK.

Zhang, L., De Schryver, P., De Gusseme, B., De Muynck, W., Boon, N., Verstraete, W., 2008. Chemical and biological technologies for hydrogen sulfide emission control in sewer systems: a review. Water Res. 42 (1–2), 1–12.

Zhang, L., Derlon, N., Keller, J., Yuan, Z., 2012. Dynamic response of sulfate-reducing and methanogenic activities of anaerobic sewer biofilms to ferric dosing. J. Environ. Eng. 138 (4), 510–517.

Zhang, L., Keller, J., Yuan, Z., 2009. Inhibition of sulfate-reducing and methanogenic activities of anaerobic sewer biofilms by ferric iron dosing. Water Res. 43 (17), 4123–4132.